Magnetic properties of YVO_3 single crystals

Y. Ren*
Solid State Physics Laboratory, Materials Science Centre, University of Groningen, Nijenborgh 4, 9747 AG Groningen, The Netherlands

T. T. M. Palstra
Inorganic Solid State Chemistry Laboratory, Materials Science Centre, University of Groningen, Nijenborgh 4, 9747 AG Groningen, The Netherlands

D. I. Khomskii
Solid State Physics Laboratory, Materials Science Centre, University of Groningen, Nijenborgh 4, 9747 AG Groningen, The Netherlands

A. A. Nugroho† and A. A. Menovsky
Van der Waals-Zeeman Institute, University of Amsterdam, Valckenierstraat 65, 1018 XE Amsterdam, The Netherlands

G. A. Sawatzky
Solid State Physics Laboratory, Materials Science Centre, University of Groningen, Nijenborgh 4, 9747 AG Groningen, The Netherlands
(Received 15 October 1999; revised manuscript received 24 March 2000)

The magnetic properties of YVO_3 single crystals have been studied in the temperature range from 350 to 4.2 K and in magnetic fields up to 7 T. It is found that in an applied field less than 4 kOe remarkable magnetization reversals occur at two distinct temperatures: an abrupt switch at $T_s = 77$ K associated with a first-order structure phase transition and a gradual reversal at $T^* \approx 95$ K without a structural anomaly. Most interestingly, the magnetization always switches to the opposite direction if the crystal is cooled or warmed through T_s and T^* in a field less than $\sim$500 Oe. In higher magnetic fields the magnetization does not change sign but has a minimum at T^* and a sudden change at T_s. A possible mechanism for the observed peculiar magnetic behavior is discussed, related to the competition of the single-ion magnetic anisotropy and the antisymmetric Dzyaloshinsky-Moriya interaction accompanied by a change of orbital ordering.

I. INTRODUCTION

Transition-metal (TM) oxides with the perovskite structure display a large variety of properties such as high-temperature superconductivity and colossal magnetoresistance. Their magnetic properties are also quite diverse, ranging from antiferro-, weak ferro-, ferri- to ferromagnetic behaviors. During the last decade, the TM oxides have been intensively reinvestigated in order to get insight into the underlying physical mechanisms and to search for new candidates with intriguing properties.

Several groups have recently reported anomalous diamagnetism occurring in the antiferromagnetic phase of $LaVO_3$ polycrystalline samples.[1–4] They have found that if a $LaVO_3$ sample is cooled in a field of 1 kOe its magnetization **M** is oriented opposite to the applied magnetic field below a temperature $T_t = 138$ K $< T_N = 144$ K. Such temperature-induced magnetic moment reversals have been observed in those ferrimagnets[5] with strong magnetic anisotropy which exhibit a compensation temperature. The net magnetization, initially oriented parallel to the field, changes sign at this temperature and the metastable energetically unfavorable state is fixed by the strong anisotropy. For such an effect to be observed, inequivalent sites must exist. Mahajan and co-workers have attributed the negative magnetization to such a ferrimagnetic behavior, since the symmetry of $LaVO_3$ changes at T_t from the orthorhombic space group $Pbnm$ to monoclinic $P2_1c$.[6] In the monoclinic phase the V ions have two crystallographically inequivalent sites. However, Goodenough and Nguyen[4] have argued that the anomalous diamagnetism is caused by a reversal of the ferromagnetic component of a canted-antiferromagnet on cooling through a cooperative, first-order magnetostrictive distortion at T_t, below which the orbital angular momentum is maximized. They suggested that the response of the orbital moment to the forces generated at the first-order phase transition can reverse the Dzyaloshinsky vector of an antisymmetric interaction so as to create a canted spin component in a direction opposite to the applied field, given that T_t is close to T_N.

Yttrium orthovanadate YVO_3 has an orthorhombically distorted perovskite structure with space group $Pbnm$, the same as the room-temperature phase of $LaVO_3$. The compound with V^{3+} $3d$ magnetic ions with spin $S = 1$ is an insulator and has several low-temperature phase transitions. Specific-heat anomalies at $T_s = 77.7$ K and $T_N = 114$ K have been reported by Boruhovich *et al.*[7] Zubkov *et al.*[8,9] have reported a neutron-diffraction study with a change in the ordered spin configuration at T_s from a low-temperature C-type antiferromagnetic (AF) phase with an AF coupling in the ab plane and a ferromagnetic coupling between two adjacent planes to a high-temperature G-type AF phase with AF couplings both in the planes and between the planes which is stable between T_s and T_N. Kawano *et al.*[10] confirm a $T_s \approx 77$ K and a Néel temperature $T_N \approx 118$ K, but they found the G-type AF phase below T_s and the C-type one between T_s and T_N with a first-order phase transition at T_s.

An anomaly in the lattice constants is observed at T_s, while no structural anomaly is found at T_N. The magnetic properties of YVO_3 and other orthovanadates have been recently investigated by Nguyen and Goodenough,[11] particularly in the light of the anomalous diamagnetism. They found no diamagnetism in YVO_3, which was confirmed by other groups.[12–14] They concluded that substitution of La by Y or Lu applies a chemical pressure that suppresses the first-order magnetostrictive distortion responsible for the anomalous diamagnetism.

We found in contrast to previous studies[7,9,11,13,14] multiple temperature-induced magnetization reversals below the Néel temperature in modest fields, no matter whether the crystal is field-cooled (FC) or zero-field-cooled (ZFC).[15] A gradual magnetization reversal occurs at about 95 K, while the magnetization reverses abruptly at 77 K associated with a first-order structural phase transition. More interestingly, the magnetization always changes sign on crossing 77 K and 95 K in modest fields. In this paper we report a detailed study of the magnetic properties of YVO_3 single crystals.

II. EXPERIMENTAL DETAILS

Single crystals of YVO_3 were made starting with powders by reduced in flowing pure H_2 at 1000 °C. YVO_4 powders were made by high-temperature solid-state reaction of appropriate mixtures of predried Y_2O_3(99.998%) and V_2O_5 (99.995%, metals basis). Single crystals with dimensions of 5 mm in diameter by 10 mm long were grown by the floating-zone method. The details about the crystal growth will be published elsewhere. Chemical analysis on the composition of the single crystals showed the cation ratio of Y over V is 1.00 ± 0.01 and the oxygen stoichiometry is 3.03 ± 0.02. Several single crystals from different batches with weight ranging from 5 to 40 mg were selected and oriented for measurements. The magnetization along different directions was measured using a Quantum Design MPMS superconducting quantum interference device system in the temperature range from 350 to 4.2 K with applied magnetic fields up to 7 T.

III. RESULTS

In Fig. 1 we illustrate the magnetization as a function of temperature for both a single crystal and a polycrystalline sample of YVO_3 after field-cooling (FC) and zero-field-cooling (ZFC). The data for the single crystal is obtained by averaging the magnetizations along the three axes. The magnetization of the FC polycrystalline sample shows no ''diamagnetic'' response but a minimum below the Néel temperature, similar to the results reported by other groups. The magnetization of the FC and ZFC samples behaves quite differently. However, the FC magnetization of the single crystal increases rapidly just below the Néel temperature $T_N = 116$ K, and then decreases monotonously after reaching a maximum. It crosses zero at $T^* \approx 95$ K and becomes negative. With further decrease in temperature, the magnetization suddenly jumps to a positive value at $T_s = 77$ K. The same behavior is also observed in a ZFC measurement, where the sample is first cooled down to 4.2 K without a magnetic field

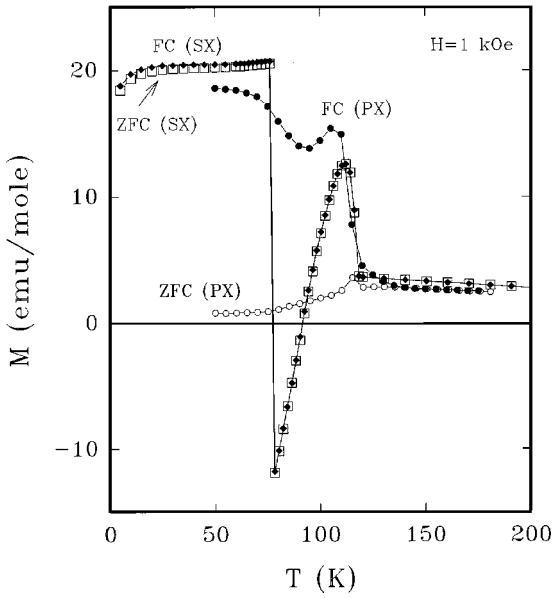

FIG. 1. Temperature dependence of the magnetization of a polycrystalline sample and single crystal in an applied magnetic field of 1 kOe. Filled and open circles are for the polycrystalline sample (PX) after field-cooling (FC) and zero-field-cooling (ZFC), respectively. Diamands and squares are for the FC and ZFC single crystal, respectively. The data for single crystal (SX) are obtained by averaging the magnetizations along the three axes.

and then a small field is applied and magnetization is measured upon warming.

The reason for the difference between the ZFC and the FC measurements of the powder samples is that in the FC the particles in the powders are magnetically annealed so that their net magnetic moments will preferentially orient in the direction of the applied magnetic field, while in the ZFC the particles will be magnetically ordered below T_N with their net moments randomly distributed. In a small field applied after the ZFC it will be hard to realign these randomly distributed moments along the field direction as in the FC. However, above a sufficiently high field there will be no difference between the ZFC and the FC. In a single crystal, e.g., with its *a* axis oriented along the field direction, the net moment will be aligned along the field direction in the FC measurements or aligned along either the positive or the negative *a* direction with the same absolute value below 77 K in the ZFC measurements. Indeed, both situations have been found in our ZFC measurements. Here only the ZFC measurements with the positive magnetization below 77 K are shown. The absence of the negative magnetization between 77 and 95 K in the powders is because this is a metastable state with the net moments opposite to the applied field direction. The particles in the powders will tend to reorient (which is not possible for the single crystals in our measurements) and/or their spins will flip (see text in the Discussion section) in order to reach the stable state with the moments along the field direction. Evidence for this particle reorientation effect is the fact that the magnetization behaves quite differently between 77 and 95 K from sample to sample and for different fields[11–14] because different sample preparations lead to powders with different particle sizes, grain-boundary conditions and also the magnetic anisotropy

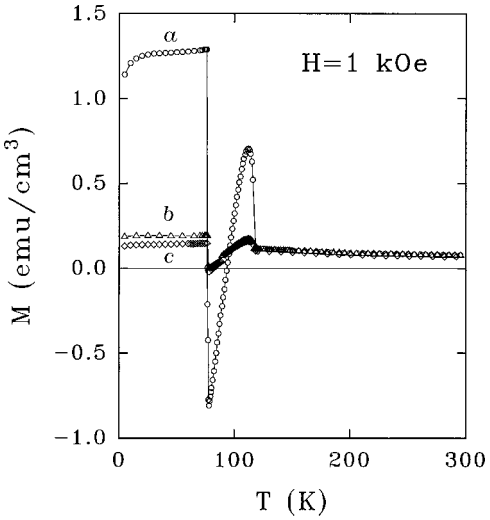

FIG. 2. Temperature dependence of the magnetization in an applied magnetic field of 1 kOe along the *a*, *b*, and *c* axis, respectively.

at the boundaries is very different from that of the bulk because of lower symmetries and different crystal-field splitting.

The magnetization along the three axes of the orthorhombic symmetry was studied, as shown in Fig. 2. It can be seen that the magnetization along the *a* axis is almost always much larger than those along the *b* and *c* axes below T_N. In further presentation of our measurements we will concentrate on the magnetic behavior along the *a* axis. In Fig. 3 the magnetization along the *a* axis in different magnetic fields is plotted versus temperature. The data for each magnetic field were measured in field cooling and then field warming. First of all the magnetization shows a clear thermal hysteresis at about T_s, indicating a first-order phase transition. Second, the sharp magnetization increase just below T_N implies a ferromagnetic component. The thermal hysteresis at T_N is also an indication of the ferromagnetic feature of the observed magnetization below T_N. In higher fields ($\gtrsim$4 kOe) the magnetization no longer becomes negative, but instead has a minimum at $T^* \approx 95$ K.

In order to understand the origin of the ''diamagnetic'' response in YVO_3, we have measured the magnetization as a function of applied field at different temperatures, as illustrated in Fig. 4. It is clear that the negative magnetization is not due to a conventional diamagnetism since the differential susceptibility dM/dH is always positive. The remanent (net) magnetic moment is $\sim$0.01 Bohr magneton per V site which for a $S=1$ system corresponds to a canting angle of $\sim 0.2°$ of the antiferromagnetic sublattice magnetizations. The magnetization reversals indicate that the net moment is aligned opposite to the applied field in certain temperature regions. The magnetic hysteresis is the same for $T=25$ and 50 K, which are below T_s. The high-field slope dM/dH at the temperatures between T_s and T_N is almost the same, while the hystereses show different remanent magnetizations and a variation of the coercive forces at different temperatures. The temperature independence of the differential susceptibility indicates that the antiferromagnetic magnetic moments are perpendicular to the applied field, i.e., to the *a* axis for both

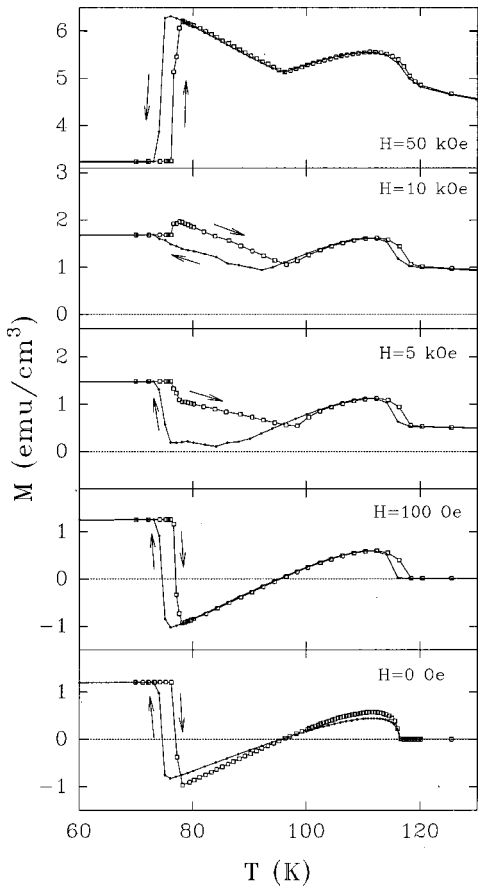

FIG. 3. Temperature dependence of the magnetization in different applied magnetic fields along the *a* axis. The curves marked by dots and squares are measured with decreasing and increasing temperature, respectively. For each field the data were measured during cooling-down and then warming-up the sample in the given magnetic field, except for $H=0$ where the nonmagnetic field was applied.

below T_s and between T_s and T_N.

In the molecular field theory of an antiferromagnet with two sublattices *A* and *B*, the molecular field $\mathbf{H}_{mA}$ acting on an atom in the sublattice *A* can be written as

$$\mathbf{H}_{mA} = -\beta_{AA}\mathbf{M}_A - \beta_{AB}\mathbf{M}_B, \tag{1}$$

where $\mathbf{M}_A$ and $\mathbf{M}_B$ are the magnetizations of the *A* and *B* sublattices, respectively, β_{AB} is a molecular field constant for the nearest-neighbor interaction, and β_{AA} is a molecular field constant for the next-nearest-neighbor interaction. The molecular field $\mathbf{H}_{mB}$ acting on an atom in the sublattice *B* can be written in the same way as for the sublattice *A* by interchanging the label *A* and *B*. For an antiferromagnet one has $\beta_{AA} = \beta_{BB}$. Using the perpendicular susceptibility for an antiferromagnet

$$\chi_\perp = \frac{1}{\beta_{AB}}, \tag{2}$$

where the single-ion anisotropy, other anisotropic interactions, and the small canting are neglected, the molecular field constants β_{AB} are calculated from Fig. 4 as $\beta_{AB} \approx 275$ K for $T < T_s$. For temperatures between T_s and T_N, β_{AB} shows a slight increase as the temperature increases, from 105 K at

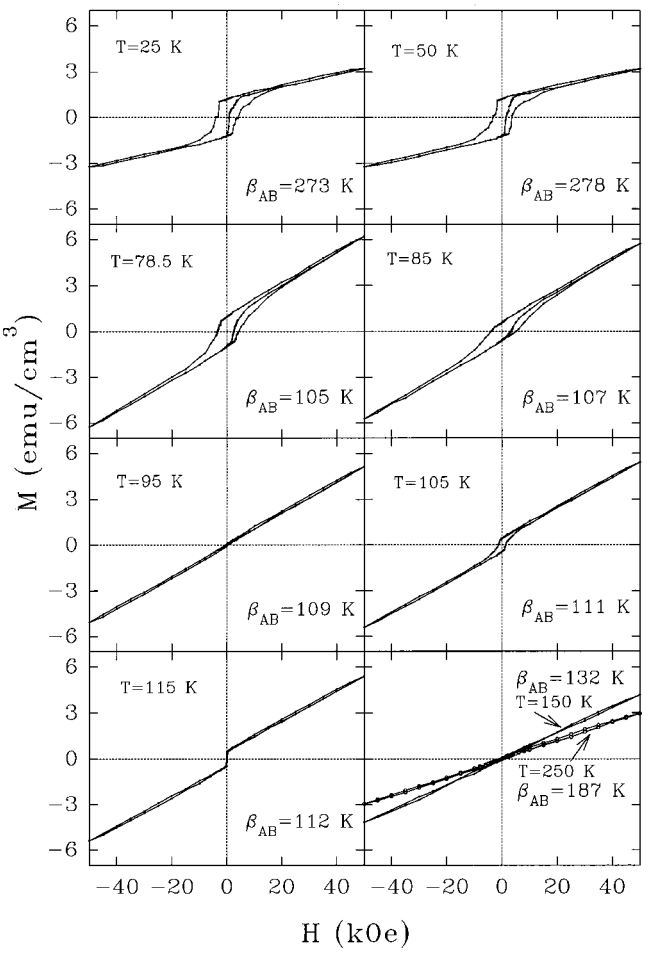

FIG. 4. The magnetization as a function of field (hystereses) at different temperatures measured with the magnetic field along the *a* axis.

78.5 K to 111 K at 114 K. This variation of β_{AB} might be due to a contribution from the magnetic anisotropy. The molecular field constant β_{AB} below T_s is about 2.5 times larger than those between T_s and T_N. This supports the neutron-diffraction results of Kawano *et al.*,[10] that the AF structure below T_s is the *G* type, while between T_s and T_N the AF structure is the *C* type. The different magnetic structures are probably a result of a change in orbital ordering as discussed below.

The different AF structures below and above T_s have been further checked by measuring the magnetization along the *c* axis as a function of field at $T=50$,78.5, and 115 K, as shown in Fig. 5. One can see that the magnetizations versus field show a linear behavior at $T=78.5$ and 115 K with the same slope which have almost the same value as obtained from the magnetic hysteresis with fields along the *a* axis (see Fig. 4). However, the high-field slope dM/dH at $T=50$ K is much smaller than the slope measured in a field along the *a* axis (Fig. 4). This indicates that the magnetic moments are aligned perpendicular to the *c* axis above T_s and parallel to the *c* axis below T_s. From Fig. 4 one can see that the sublattice magnetic moments are almost perpendicular to the *a* axis both below and above T_s. Thus, the *G*-type AF structure below T_s has magnetic easy axes almost along the *c* axis, while the *C*-type one above T_s has the easy axes almost along the *b* axis.

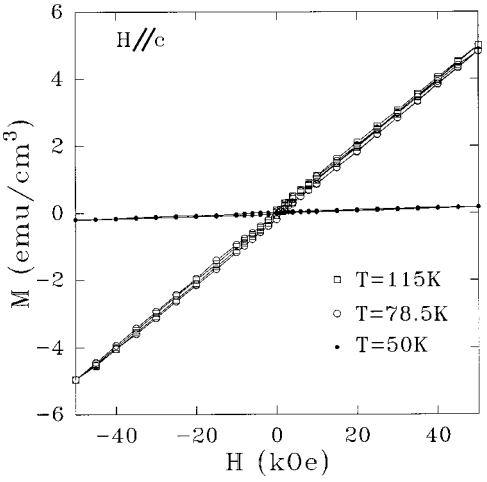

FIG. 5. The magnetization as a function of field (hystereses) at different temperatures measured with the field along the *c* axis.

Besides the multiple magnetization reversals below the Néel temperature T_N, the susceptibility above T_N shows a change at $T_o \approx 200$ K, as shown in Fig. 6 where the susceptibility and inverse susceptibility measured along the *a* axis are plotted as a function of temperature together with fits using the Curie-Weiss relation, $\chi = C/(T+\theta_{CW})$. Above T_o the effective moment for the V ions is $p_{\text{eff}}=2.814(2)$ as expected for the spin $S=1$, and $\theta_{CW}=234(4)$ K. One finds $\theta_{CW}/T_N \approx 2$. Using the molecular field theory expression

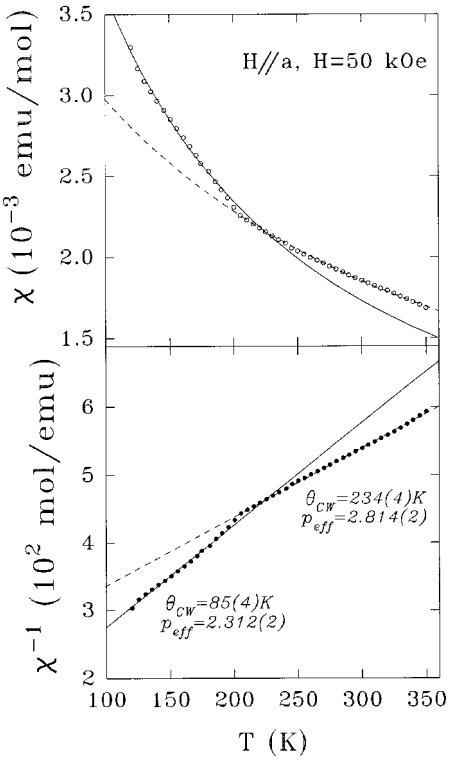

FIG. 6. Temperature dependence of the susceptibility (open circles) and inverse susceptibility (filled circles) above the Néel temperature. The Curie-Weiss law $\chi = C/(T+\theta)$ with $C = Np_{eff}^2\mu_B^2/3k_B$ is used to fit the observed data. The solid and dashed lines are calculated from the fits for the susceptibility below and above 200 K, respectively.

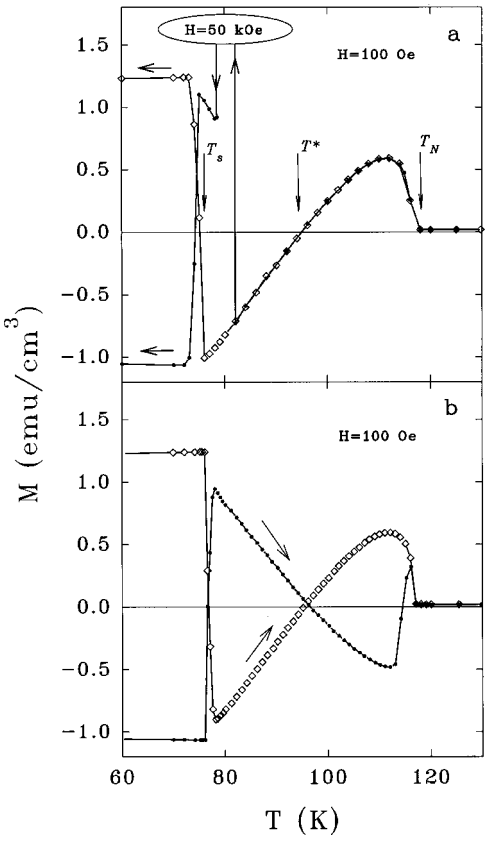

FIG. 7. Magnetization versus temperature in a field of 100 Oe, exhibiting the memory effect upon the application of large fields. In the curve marked by filled circles in panel **a** we follow **M** with decreasing temperature down to a temperature below T^*; a high field is then applied to flip the magnetization positive after which the field is lowered again to 100 Oe and the temperature decreases. The curve marked by diamonds is measured without intermediate application of the high field. In panel **b** we show the curves with increasing temperature starting from below T_s: the curve marked by diamonds without having ''trained'' the sample, and the curved marked by filled circles after ''training'' as described in panel **a**.

$$\frac{\theta_{CW}}{T_N}=\frac{\beta_{AB}+\beta_{AA}}{\beta_{AB}-\beta_{AA}}, \tag{3}$$

one obtains $\beta_{AB}/\beta_{AA}\approx 3$. But below T_o $p_{\text{eff}}=2.312(2)$ and $\theta_{CW}=85(4)$ K using the Curie-Weiss relation to analyze the data. Although the Curie-Weiss relation may be too simple, the decrease in p_{eff} may be a sign of an increasing importance of the spin-orbital coupling. For a less than half-filled d shell we expect the orbital moment to be oriented antiparallel to the spin moment.

From Fig. 4 one can see that the negative magnetization between T^* and T_s can be changed to positive by applying a high field and then releasing the field. Figure 7 shows how the magnetization behaves after such ''training.'' In the curve marked by dots in Fig. 7(a) we follow **M** with decreasing temperature down to a temperature below T^*; a high field of 50 kOe is then applied to flip the magnetization positive after which the field is lowered again to 100 Oe and the temperature decreases. The magnetization, made parallel to the field by such a treatment, then changed to antiparallel to the field below T_s. The curve marked by open diamonds

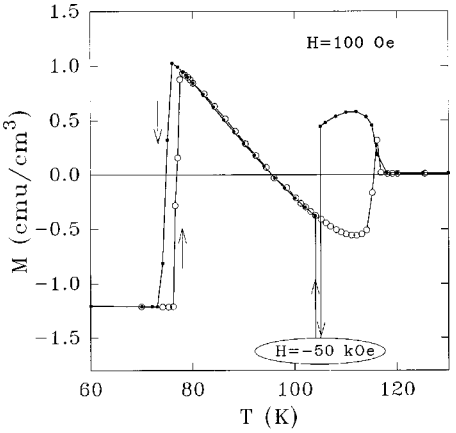

FIG. 8. Magnetization versus temperature in a field of 100 Oe with a ''training'' at $T=105$ K$>T^*$. In the curve with filled circles we follow **M** with decreasing temperature down to $T=105$ K; a high negative field of -50 kOe is then applied to flip the magnetization negative after which the field is changed to 100 Oe again and the temperature decreases. The curve with open circles is measured upon warming after the temperature is below T_s. This shows the same behavior as demonstrated in Fig. 8.

is measured without intermediate application of the high field. In Fig. 7(b) we show the behavior of magnetization with increasing temperature starting from below T_s: the open diamond marked curve is measured without having ''trained'' the sample, and the dotted curve after ''training'' as described in Fig. 7(a). This demonstrates the reversiblility: upon warming the sample after training, the temperature-dependent magnetization $\mathbf{M}(T)$ now switches from negative below T_s to positive for $T_s<T<T^*$ and becomes negative for $T>T^*$. It is thus nearly a ''mirror image'' of the curves for the untrained sample marked by the open diamonds except becoming positive again close to T_N. Such a ''training'' can be performed at any temperatures below T_N. Figure 8 demonstrates the memory effect of the magnetization after a ''training'' at $T=105$ K using a high field of -50 kOe. However, the temperature-dependent magnetization after a ''training'' is strongly dependent on the magnetic field subsequently applied for the magnetization measurements, as illustrated in Fig. 9. If a field of 500 Oe is applied after ''training'' the magnetization can still reverse on crossing T_s [Fig. 9(a)]. But the negative magnetization is only about -0.3 emu/cm^3, instead of -1.1 emu/cm^3 for the field of 100 Oe (see Fig. 8). If a field of 1 kOe is applied after the ''training,'' the magnetization can no longer switch to negative below T_s [Fig. 9(b)], but instead jumps to an intermediate state with a magnetization of about 0.7emu/cm^3 which is about half the magnitude of the magnetization in $H=100$ Oe (see Fig. 8). With increasing temperature the magnetization behaves similarly as without ''training,'' except that the magnetization switches to negative at T_s with an intermediate value and becomes positive at a lower temperature than $T^*\approx 95$ K. The intermediate state may be due to partial reversal of magnetic moments caused by a high field.

IV. DISCUSSIONS

From the data presented here, especially those of Fig. 4, it is clear that we are dealing here with weak ferromagnetism,

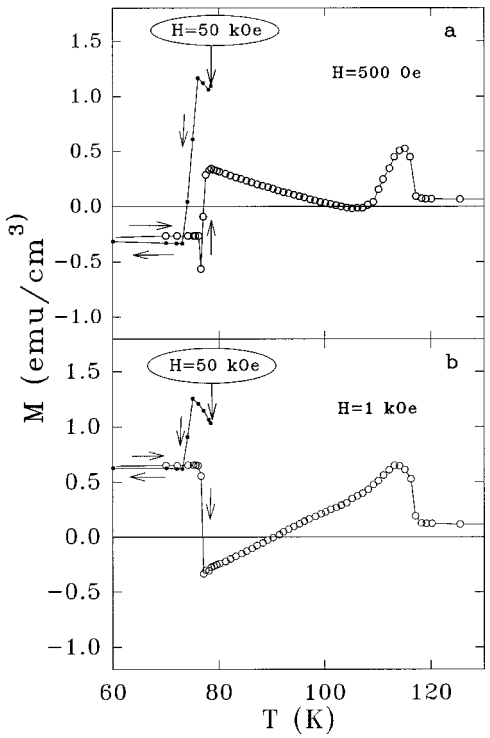

FIG. 9. Magnetization versus temperature in a field of 500 Oe and 1 kOe, respectively, after a ''training'' at $T=78.5$ K using a high field of 50 kOe. The curves with filled circles are measured with decreasing temperature after the ''training.'' The curves with open circles are measured upon warming from temperature below T_s following the curves with filled circles.

caused by a departure from the strict collinearity of the magnetic moments in an antiferromagnet. There are two mechanisms giving rise to a canting of the antifferromagnetic alignment of spins: the single ion magnetic anisotropy and the antisymmetric spin-spin interaction. The latter was obtained by Dzyaloshinsky in a phenomenological analysis of α-Fe_2O_3 and other compounds.[16] He showed that in the free energy of the system in terms of the sublattice magnetizations there is an important term

$$\mathbf{D}\cdot(\mathbf{M}_1\times\mathbf{M}_2), \tag{4}$$

where $\mathbf{D}$ is a vector (so-called Dzyaloshinsky vector) and $\mathbf{M}_1$ and $\mathbf{M}_2$ are the magnetic moments of the two sublattices, respectively. This coupling favors a perpendicular orientation of the two sublattice magnetizations. This coupling is generally very small compared to the Heisenberg exchange interaction $J\vec{S}_1\cdot\vec{S}_2$ which prefers collinear spin arrangements. When this coupling is introduced to the antiferromagnetic crystal, a canting of the sublattice magnetizations takes place. The microscopic origin of this term has been studied by Moriya and was attributed to the antisymmetric superexchange interaction including spin-orbital coupling.[17,18] Moriya calculated the tensor describing anisotropic superexchange interaction of two neighboring spins $\vec{S}_1$ and $\vec{S}_2$ and showed that it contains an antisymmetric term

$$\mathbf{d}_{12}\cdot(\vec{S}_1\times\vec{S}_2), \tag{5}$$

where $\mathbf{d}_{12}$ is the Moriya one-bond vector, which is *zero* if the anion mediating the superexchange interaction between the two neighboring magnetic ions is sitting at an inversion center.

YVO_3 has an orthorhombically distorted pervoskite structure with space group $Pbnm$. The distorted crystal structure with tilted VO_6 octahedra quite naturally leads to canted spin structures. First, since the oxygen ions mediating the superexchange interaction between two nearest-neighbor V ions are not at an inversion center the antisymmetric interaction will be present. Also because the VO_6 octahedra are tilted forming a staggered V-O bond direction the single-ion anisotropy easy axis is staggered. Each of the two mechanisms may lead to weak ferromagnetism.[19] From Fig. 2 one can see that the largest magnetization is almost always along the *a* axis, which indicates that both canting mechanisms produce the net magnetic moment along the same axis, i.e., the *a* axis; this is usually the case when both mechanisms are present simultaneously. However, they need not have the same sign, and, besides, they may be temperature dependent. A competition of the two mechanisms has been suggested by Goodenough and Nguyen[4,11] and Corti *et al.*[14] This is the essence of an explanation of the magnetization switching which we propose: the competition between these two mechanisms leads to the magnetization reversals, because different mechanisms dominate in different temperature intervals.

The Hamiltonian of the magnetic system in an external field can be written in the form:

$$\mathcal{H}=\mathcal{H}_a+\mathcal{H}_s+\mathcal{H}_e, \tag{6}$$

where the three terms are for the single-ion anisotropy, the spin-spin interaction and the external field, respectively. In a small field the last term can be neglected. The antiferromagnetic structure in YVO_3 between T_s and T_N can be described in two sublattices, *A* and *B* with an equal number *N*, of V ions per sublattice. Assuming a uniaxial magnetic single ion anisotropy, the term $\mathcal{H}_a$ can be expressed as

$$\mathcal{H}_a=-\sum_{i=1}^{N}A_AS_{i,z_A}^2-\sum_{j=1}^{N}A_BS_{j,z_B}^2=-N(A_AS_{z_A}^2+A_BS_{z_B}^2), \tag{7}$$

where A_A and A_B are the single-ion anisotropies for the V ions in the sublattice *A* and *B* respectively, which are equal $A_A=A_B=A$, and the subscript z_A and z_B denote the local easy axis for the spins in the two sublattice *A* and *B*, respectively.

Considering the nearest-neighbor (NN) interaction of V^{3+} spins, one has

$$\begin{aligned}\mathcal{H}_s&=-\sum_{\langle ij\rangle}[J_{ij}\mathbf{S}_i\cdot\mathbf{S}_j-\mathbf{d}_{ij}\cdot(\mathbf{S}_i\times\mathbf{S}_j)-\mathbf{S}_i\cdot T_{ij}\cdot\mathbf{S}_j]\\&=-N[n_aJ_a\mathbf{S}_A\cdot\mathbf{S}_B+\mathbf{D}\cdot(\mathbf{S}_A\times\mathbf{S}_B)+\mathbf{S}_A\cdot T\cdot\mathbf{S}_B]+\mathcal{H}_f,\end{aligned} \tag{8}$$

where the J_{ij} is the isotropic symmetric exchange coupling constant between the two spins *i* and *j*, and the $\mathbf{d}_{ij}$ and T_{ij} are the antisymmetric exchange and symmetric anisotropies, respectively. J_a is the antiferromagnetic coupling constant, n_a the number of the NN antiferromagnetic couplings of a V^{3+}

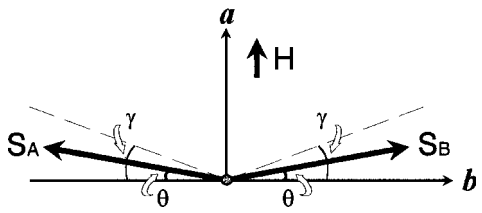

FIG. 10. Schematic drawing of the canting of two sublattice magnetizations $\mathbf{S}_A$ and $\mathbf{S}_B$.

ion. $\mathbf{D}$ and T are the summations of $\mathbf{d}_{ij}$ and T_{ij} over the nearest noughbours of a spin. $\mathbf{S}_A$ and $\mathbf{S}_B$ are the spins in the sublattice A and B, respectively. $\mathcal{H}_f$ is a contribution from the weakly ferromagnetic NN couplings.

According to the analysis of Shekhtman *et al.*[20] in the case of La_2CuO_4, the symmetric anisotropy T is of the order $\sim|D|^2/4J$ in the free-energy expression. In our model the term T will be omitted since it does not play any quantitatively important role in determining the temperature dependence of the canting angle. Our magnetic study of YVO_3 (Ref. 15) implied that the single-ion anisotropy and the antisymmetric interaction prefer the net moment in the opposite directions. It is assumed that the single ion anisotropies prefer the spins along the dashed lines with a canting angle γ as shown in Fig. 10, and that the antisymmetric interaction prefers to cant the spins in the opposite direction with the Dzyaloshinsky vector $\mathbf{D}$ pointing into the plane. Combining the Eqs. (7) and (8) the energy of the system can be written as

$$E/N=-2AS_z^2+J\mathbf{S}_A\cdot\mathbf{S}_B+\mathbf{D}\cdot(\mathbf{S}_A\times\mathbf{S}_B)+E_f/N, \qquad (9)$$

where $J=n_a|J_a|$, $S_z=S_{z_A}=S_{z_B}$ and E_f is the NN ferromagnetic interaction which does not depend on the canting angle. In the canted antiferromagnetic system with a canting angle θ, the sublattices spins $\mathbf{S}_A$ and $\mathbf{S}_B$ are almost antiparallel, giving rise to two almost antiparallel sublattice magnetizations with the same absolute value $Ng\mu_B|\langle\mathbf{S}\rangle|$. Thus Eq. (9) becomes

$$E/N=-2AS^2\cos^2(\theta-\gamma)-J|\langle\mathbf{S}\rangle|^2\cos(2\theta)+D|\langle\mathbf{S}\rangle|^2\sin(2\theta)+E_f/N, \qquad (10)$$

where $D=|\mathbf{D}|$. By minimizing the energy we get

$$2AS^2\cos(\theta-\gamma)\sin(\theta-\gamma)+J|\langle\mathbf{S}\rangle|^2\sin(2\theta)+D|\langle\mathbf{S}\rangle|^2\cos(2\theta)=0. \qquad (11)$$

From the magnetic measurements of YVO_3, we know $\theta\sim\gamma<<1$. Therefore the sine and cosine functions can be replaced by the first terms of the Taylor expansions, and Eq. (11) gives

$$\theta=\frac{2AS^2\gamma-D|\langle\mathbf{S}\rangle|^2}{2AS^2+2J|\langle\mathbf{S}\rangle|^2}. \qquad (12)$$

By introducing $\xi=A/J$ and $\gamma_D=D/2J$, and since $S=1$ for YVO_3, the above equation becomes

$$\theta=\frac{\xi\gamma-\gamma_D|\langle\mathbf{S}\rangle|^2}{\xi+|\langle\mathbf{S}\rangle|^2}. \qquad (13)$$

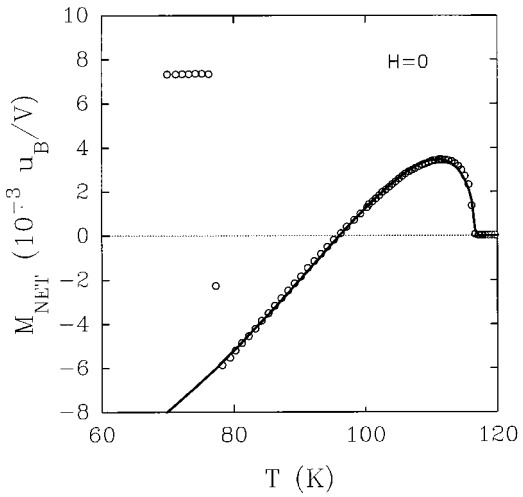

FIG. 11. Temperature dependence of the net magnetic moment along the a axis of a YVO_3 single crystal. The circles are observed data and the solid line is calculated using the equation with fit parameters (see text).

The net moment of the canted AF system is

$$M_{net}=2Ng\mu_B|\langle\mathbf{S}\rangle|\sin(\theta)\approx 2Ng\mu_B|\langle\mathbf{S}\rangle|\,\theta=2Ng\mu_B|\langle\mathbf{S}\rangle|\frac{\xi\gamma-\gamma_D|\langle\mathbf{S}\rangle|^2}{\xi+|\langle\mathbf{S}\rangle|^2}. \qquad (14)$$

Using the mean-field theory to calculate the temperature dependence of the sublattice magnetizations $M=Ng\mu_B|\langle\mathbf{S}\rangle|$, a very good description is obtained of the behavior between T_s and T_N as shown in Fig. 11, in which the solid curve calculated using the fit parameters $\xi=A/J=1.7(1)$, $\gamma=7.56(8)\times10^{-3}$ and $\gamma_D=D/2J=31(2)\times10^{-3}$, describes all the features of the temperature-dependent net magnetic moment in that temperature region. The coupling constant $J=174$ K can be calculated from the mean-field equation ($S=1$):

$$J=n_aJ_a=\frac{3k_BT_N}{S(S+1)}. \qquad (15)$$

The fit parameter, $\xi=A/J=1.7$, indicates a large single-ion anisotropy, $A\approx296$ K (~25 meV). This is surprising at first glance, but we should recall that the spin-orbit coupling of V is about 20 meV or 200 K and for a small non cubic crystal field would split the t_{2g} orbits into a doublet and a singlet with a splitting which could also be of order 200 K. In this situation a magnetic anisotropy of order 200 K is not unexpected. We should also note that for such a large magnetic anisotropy it is no longer accurate to neglect it in calculating the temperature dependence of the sublattice magnetization as we did. A more detailed analysis including also a microscopic calculation of D and A is under way and will be published elsewhere. We note that the situation encountered in YVO_3 is probably quite different from standard examples like V^{+3} impurities in Al_2O_3.[21] In the later case the distortion from cubic symmetry is trigonal and the orbital singlet is the lowest in energy with a noncubic crystal field an order of

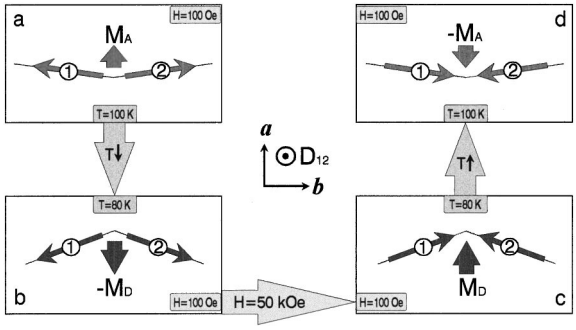

FIG. 12. Pictorial view of the temperature dependence of the magnetization: (a) Just below T_N the two sublattice spins prefer to lie close to a local easy axis, if the local magnetic anisotropy is large, resulting in a net magnetic moment parallel to the applied field. (b) As T decreases below $T^*=95$ K the DM interaction dominates which tends to cant the spins in opposite direction. A large external magnetic field can overcome the barrier for rotation of the sublattice spins, resulting in a reversal of the sublattice spin orientation. (c) The net moment is now oriented parallel to the field and will remain so upon lowering the field. If we now increase the temperature we will come back to the situation where the magnetic anisotropy dominates. (d) Thus, the net moment will change sign again, now turning negative for $T>95$ K.

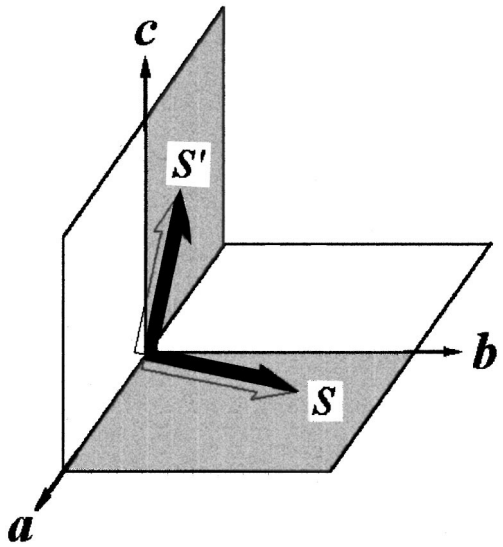

FIG. 13. Pictorial illustration of how the spins reconstruct on crossing the first order phase transition temperature T_s. The vector **S** is lying close to the b axis with a small positive canting angle towards to the a axis in the ab plane. The vector **S**′ is in the ac plane with a small nagetive canting angle towards the negative a axis.

magnitude larger than the spin-orbit coupling. This leads to a magnetic anisotropy an order of magnitude smaller than what we find in YVO_3.

The theoretical model developed here permits also to explain the phenomenon of ''training'' observed above. We present in Fig. 12 a pictorial view of this model to illustrate what could happen microscopically as a function of temperature. We start in Fig. 12(a) at temperatures just below T_N. Here, the two sublattice spins will prefer to lie close to a local easy axis due to local magnetic anisotropy, resulting in a net magnetic moment along the applied field as shown. As T decreases this net moment will first grow because of the development of a sublattice magnetization due to superexchange. However, as the sublattice magnetization develops, so does the antisymmetric coupling which tends to cant the spins in the opposite direction. Consequently, with decreasing temperature the net moment will reach a maximum and then decrease. It crosses zero at the temperature below which the antisymmetric interaction dominates. This will result in a moment opposite to the small applied field. It could only reverse to its lowest energy state in the field by reversing the two sublattices on a macroscopic scale, resulting in a frozen metastable state [Fig. 12(b)]. A large external magnetic field can overcome the barrier for rotation of the sublattice spins, resulting in a reversal of the sublattice spin orientation [Fig. 12(c)]. The net moment is now oriented parallel to the field and will remain so upon lowering the field. If we now increase the temperature we will come back to the situation where the magnetic anisotropy dominates. Thus, the net moment will change sign again, now turning negative for $T>95$ K [Fig. 12(d)]. Once we get close enough to T_N, the energy barrier for the reversal of the sublattice magnetizations will eventually become very small. Any finite field will now flip the net moment again to a positive value, and reach a maximum just below T_N dropping to zero at T_N [Fig. 7(b)]. This model explains all the data from high temperatures down to the first order phase transition at $T_s=77$ K.

We note that in general the magnetic anisotropy is taken to be proportional to the sublattice magnetization squared and therefore would be strongly temperature dependent. This, however, is not the correct approach if the dominant term is of a single-ion nature. Clearly such a contribution to the magnetic anisotropy depends only on the angle the spin makes with the easy axis and the long range order itself is of no direct consequence. Clearly if we would have taken the anisotropy energy to be related directly to the sublattice magnetization we would have required strong temperature dependent constants A and D to explain the results. However, by treating the anisotropy energy correctly we can easily explain the results without any additional parameters. The often strong temperature dependences of the magnetic anisotropies found in the literature could in many cases be related to an incorrect treatment of the temperature dependence of the anisotropy energy.

The magnetization reversal at T_s remains more of a puzzle. As follows from our data, the ferromagnetic moment is oriented along the a axis both above and below T_s, and the magnetic easy axis is almost along the c axis below T_s and along the b axis above T_s. From the neutron-scattering results recently obtained we know that the magnetic structure changes at T_s, from C- to G-type as originally proposed by Kawano *et al.*[10] This is consistent with the consideration from the symmetry point of view.[19] For the orthorhombic space group $Pbnm$ to which YVO_3 belongs, the spin configuration F_a with a ferromagnetic moment along a can only coexist with either the mode G_c or C_b in the presence of magnetic anisotropy, where the G_c-type magnetic structure has the easy axis close to the c axis and the easy axis of the C_b-type one is close to the b axis. Figure 13 illustrates how a spin changes its direction on crossing T_s. The spins are lying in the ab plane for the C-type AF ordering above T_s

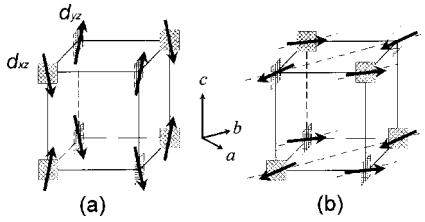

FIG. 14. Suggested orbital ordering below and above $T_s = 77$ K: (a) a *C*-type orbital ordering with a *G*-type spin ordering; and (b) a *G*-type orbital ordering with a *C*-type spin ordering. The dotted lines are along the *b* axis. The hatched squares indicate the planes in which the occupied *d* orbitals lie. The d_{xy} orbitals which are in each case occupied by one electron are omitted for clarity.

and in the ac plane for the *G*-type one below T_s. If a spin, say labeled as **1**, above T_s lies along the **S** direction as shown in Fig. 13 with a *positive* net moment along the *a* axis, below T_s it will be either along the $\mathbf{S}'$ direction or along the direction of a mirror imagine of $\mathbf{S}'$ with the ab plane as a mirror, which is denoted as $\tilde{\mathbf{S}}'$, with a *negative* net moment along the $-a$ axis. Once the spin **1** is rotating from S to S' on crossing T_s, its six neighboring spins, among which four spins in the ab plane have AF coupling and two along the *c* axis have ferromagnetic coupling, will all rotate to the $\tilde{\mathbf{S}}'$ direction giving rise to the *G*-type spin configuration. But if the spin **1** lies in the opposite direction of **S** above T_s it will orient along the opposite direction of either $\mathbf{S}'$ or $\tilde{\mathbf{S}}'$.

The change of spin structure associated with a first-order phase transition is definitively connected with a change of orbital ordering occurring at T_s. Our recent low-temperature single crystal x-ray diffraction and neutron powder-diffraction studies of YVO_3 show that whereas above T_s two pairs of long (2.023 and 2.015 Å) V-O bonds in the basal ab plane are almost equal and one pair of short bonds of 1.982 Å is along the *c* direction, the first order phase transition is accompanied by a strong distortion of these bond lengths resulting in long (2.052 Å), intermediate (1.992 Å) and short (1.975 Å) V-O bonds. The long and short bonds are oriented alternately along the $[110]$ and $[1\bar{1}0]$ directions in the basal ab plane while the intermediate one of 1.992 Å is along the *c* axis, similar to the structure of $LaMnO_3$. Such a distortion corresponds to an orbital ordering, with the d_{xy} orbital occupied at each V^{3+} site and the second electron occupying, respectively, d_{xz} and d_{yz} orbitals in two sublattices as shown in Fig. 14. According to the Goodenough-Kanamori rules[22] this orbital occupation naturally leads to the *G*-type antiferromagnetism.[10] According to Bertaut's symmetry considerations the easy axis of the *G*-type ordering is close to the *c* direction in order for the net weak moment to lie along the *a* axis. This scenario is confirmed by our data (Figs. 4 and 6). A similar result was also obtained by band-structure calculation.[23,24] The magnetic structure above T_s is of *C* type with the easy axis close to the *b* direction. From this we conclude that the easy axis must indeed change on going through the phase transition. The *C*-type magnetic ordering observed between T_s and T_N should then correspond to an orbital structure with the alternation of the orbital sublattices also along the *c* direction and, as discussed above, with the easy axis almost $\|b$. Such an orbital ordering is observed for $LaVO_3$ at temperature below $T_t = 138$ K.[6] From our magnetic measurements we argue that most probably this orbital ordering occurs at a temperature well above the Néel temperature T_N, namely, at $T_o \approx 200$ K. This is supported by our low-temperature x-ray single crystal study which shows that the lattice parameters have an anomaly at T_o but behave smoothly at T_N. Thermal expansion study of YVO_3 also shows little coupling between the AF ordering and the lattice at T_N while a change definitely occurs at T_o.[25] However, there is still no clear evidence for such a ''*C*-type'' orbital ordering between T_s and T_o from the crystal structure point of view. Detailed investigation of this orbital ordering will be carried out using x-ray scattering facilities.

V. CONCLUSIONS

The magnetic properties of YVO_3 single crystals have been studied. We found a magnetic behavior for this compound: multiple and reversible sign changes of the magnetization with temperature, resulting in a temperature range where the magnetic moment is oriented in a direction *opposite* to the applied magnetic field. The net magnetization is caused by a canting of the nearly antiferromagnetic arrangement of the spins of the magnetic V^{+3} ions with $S = 1$ below the Néel temperature $T_N = 116$ K. In a field less than 4 kOe with decreasing temperature the net moment increases rapidly to a maximum below T_N and then decreases monotonously to negative values after crossing $T^* \approx 95$ K. At $T_s = 77$ K the net moment switches to positive again. A first-order phase transition at T_s is confirmed by a clear hysteretic change of a magnetization as a function of temperature. Furthermore, we report a memory effect of the magnetization: the net moment always switches from positive to negative, or vice versa, on going through T_s and T^* in small fields. We present a theoretical model to explain the observed phenomena between T_s and T_N. It includes the competition between the single ion anisotropy and the antisymmetric interaction. It is found that the magnetic structures below and above T_s are strongly interdependent via a change of orbital orderings at T_s: the magnetic structure switches from the *C*-type to the *G*-type with a simultaneous change of orbital ordering from the *G* type to the *C* type, and during the change a spin reorientation occurs in such a way that the net moment always changes its sign.

ACKNOWLEDGMENTS

We thank J. B. Goodenough for numerous detailed discussions of the results and for the explanations of his ideas concerning the origin of the magnetization reversal in $LaVO_3$. We also thank J. Rodriquez-Carvajal, E. F. Bertaut, and B. Büchner for useful discussions. This work was supported by the Netherlands Foundation for the Fundamental Research of Matter (FOM) with financial support from the Dutch Organization for the Advancement of Pure Research (NWO), and also supported in part by EC (OXSEN).

*Present address: Argonne National Laboratory, MSD, Building 223, Argonne, Illinois 60439.
†On leave from Jurusan Fisika, Fakultas Matermatika dan Ilmu Pengetahuan Alam, Institut Teknologi Bandung, Indonesia.

[1] A.V. Mahajan, D.C. Johnston, D.R. Torgeson, and F. Borsa, Physica C **185-189**, 1195 (1991).
[2] A.V. Mahajan, D.C. Johnston, D.R. Torgeson, and F. Borsa, Phys. Rev. B **46**, 10 966 (1992).
[3] N. Shirakawa and M. Ishikawa, Jpn. J. Appl. Phys., Part 2 **30**, L755 (1991).
[4] J.B. Goodenough and H.C. Nguyen, C. R. Acad. Sci., Ser. IIb: Mec., Phys., Chim., Astron. **319**, 1285 (1994).
[5] N. Menyuk, K. Dwight, and D.G. Wickham, Phys. Rev. Lett. **4**, 119 (1960).
[6] P. Bordet, C. Chaillout, M. Marezio, Q. Huang, A. Santoro, S.-W. Cheong, H. Takagi, C.S. Oglesby, and B. Batlogg, J. Solid State Chem. **106**, 53 (1993).
[7] A.S. Borukhovich, G.V. Bazuev, and G.P. Shveikin, Fiz. Tverd. Tela (Leningrad) **16**, 286 (1974) [Sov. Phys; Solid State **16**, 191 (1974)].
[8] V.G. Zubkov, A.S. Borukhovich, G.V. Bazuev, I.I. Matveenko, and G.P. Shveikin, Zh. Éksp. Teor. Fiz. **66**, 1823 (1974) [Sov. Phys. JETP **39**, 896 (1974)].
[9] V.G. Zubkov, G.V. Bazuev, and G.P. Shveikin, Fiz. Tverd. Tela (Leningrad) **18**, 2002 (1976) [Sov. Phys. Solid State **18**, 1165 (1976)].
[10] H. Kawano, H. Yoshizawa, and Y. Ueda, J. Phys. Soc. Jpn. **63**, 2857 (1994).
[11] H.C. Nguyen and J.B. Goodenough, Phys. Rev. B **52**, 324 (1995).
[12] J. Kikuchi, H. Yasuoka, Y. Kokubo, and Y. Uda, J. Phys. Soc. Jpn. **63**, 3577 (1994).
[13] F. Cintolesi, M. Corti, A. Rigamonti, G. Rossetti, P. Ghigna, and A. Lascialfari, J. Appl. Phys. **79**, 6624 (1996).
[14] M. Corti, F. Cintoesi, A. Lascialfari, A. Rigamonti, and F. Rossetti, J. Appl. Phys. **81**, 5286 (1997).
[15] Y. Ren, T.T.M. Palstra, D.I. Khomskii, E. Pellegrin, A.A. Nugroho, A.A. Menovsky, and G.A. Sawatzky, Nature (London) **396**, 441 (1998).
[16] I. Dzyaloshisky, J. Phys. Chem. Solids **4**, 241 (1958).
[17] T. Moriya, Phys. Rev. **117**, 635 (1960).
[18] T. Moriya, Phys. Rev. **120**, 91 (1960).
[19] E. F. Bertaut, in *Magnetism*, Vol. III, edited by G. T. Rado and H. Suhl (Academic, New York, 1963), pp. 86–126.
[20] L. Shelktman, A. Aharony, and O. Entin-Wohlman, Phys. Rev. B **47**, 174 (1993).
[21] A. Abragam and B. Bleaney, *Electron Paramagnetic Resonance of Transition Ions* (Clarendon, Oxford, 1970).
[22] J.B. Goodenough, Prog. Solid State Chem. **5**, 145 (1963).
[23] H. Sawada, N. Hamada, K. Terakura, and T. Asada, Phys. Rev. B **53**, 12 742 (1996).
[24] H. Sawada and K. Terakura, Phys. Rev. B **58**, 6831 (1998).
[25] B. Buechner, Y. Ren, and G. A. Sawatzky (unpublished).